PAPER

Check for updates

Predicting power plant emissions using public data and machine learning†

Jiajun Gu, Jeffrey A. Sward [ID] and K. Max Zhang* [ID]

Accurately predicting emissions from electric generating units using only publicly available information is an important but challenging task. It provides a critical link in evaluating the environmental impact of energy transitions in the power sector, makes it possible to engage stakeholders in electricity product cost modeling and electricity markets without accessing proprietary data, and serves as an auditing tool to detect anomalies in self-reported emissions data. However, the absence of proprietary data also limits the prediction accuracy. In this paper, we adopted two novel and effective strategies to overcome this challenge. First, we utilized not only the emission monitoring data (such as the Continuous Emission Monitoring System (CEMS) data) as previous studies did but also a variety of auxiliary datasets in the public domain such as the EPA Field Audit Checklist Tool (FACT). Second, we employed machine learning techniques (Extreme gradient boosting (XGBoost) and neural networks (NN)) to take advantage of the large amount of public data available. We evaluated the effectiveness of our strategies by predicting NO_x, SO_2, and CO_2 emission rates for all thermal electric generating units in New York State (NYS). Two models were developed: a full model to take a full inventory of public information and a reduced model for use in data-limited scenarios based on unit-level features that could be derived from a simplified power systems economic dispatch model. The models performed well for NO_x emission rates overall compared to the previous results, achieving R^2 values over 0.9 for both the full and reduced models. XGBoost and NN were shown to outperform the Linear Regression (LR) model consistently and significantly, which was employed previously to estimate unit-level emissions, especially in reduced models with a limited number of features available. The predictions of SO_2 and CO_2 emission rates showed strong overall predictive performance as well. We recommend stricter enforcement of the data reporting procedure, providing emission control operational information, and obtaining related data from multiple sources in the public domain as key steps to further improve the emission predictions.

Environmental significance

Predictive models of electric generating units' emissions are widely used in important energy and environmental applications. Models using only publicly available information have many societal benefits but often result in poor performance due to the lack of proprietary data. We tested two novel strategies, including (1) utilizing previously ignored but valuable public datasets on EGU operations to complement the emission data and (2) employing non-linear machine learning techniques compared to the traditional linear regression approach, to enhance the performance and showed that our models out-performed the previous ones consistently and significantly in predicting NO_x, SO_2, and CO_2 emission rates. Therefore, we were able to present the most accurate open-accessible EGU emission prediction models for researchers, practitioners, and policymakers.

1 Introduction

The power sector worldwide is currently in the midst of a rapid transition. For example, the fractions of the electricity generated in the U.S. from coal-fired and natural gas-fired power plants were 50% and 19% in 2015 as compared to 19% and 40% in 2020, respectively, according to the Energy Information

Sibley School of Mechanical and Aerospace Engineering, Cornell University, Ithaca, NY 14853, USA. E-mail: kz33@cornell.edu

Agency (EIA). Renewables dominated new electricity generation capacity added in 2020, consisting of wind (44%), solar (31%), and natural gas (22%). Since the power sector contributes substantially to emissions of greenhouse gases, criteria pollutants, and air toxics, these changes in the fuel mix improve air quality and mitigate climate change. The state-of-the-art method for assessing the air quality and health impacts of power system changes (such as high penetration of renewable energy) relies on linking a power systems unit commitment (UC) and economic dispatch (ED) model to a regional air quality model (*e.g.*, CMAQ). One component crucial to this linkage is a prediction of electric generating unit (EGU) emissions (*i.e.*,

hourly, by pollutant type, for each EGU) given power dispatch profiles. In addition, a good emission prediction model is necessary for the economic environmental dispatch (EED) of generators, which minimizes both generation and environmental costs.

Furthermore, as emission monitoring and control contributes to an increasing share of the EGU operational costs, the capacity to accurately predict EGU emissions can greatly improve electric production cost modeling, which is critical to ensuring efficient and reliable power system operations.[1] Moreover, predicting EGU emissions using data in the public domain is particularly valuable because it makes broader stakeholder engagement possible by avoiding proprietary data internal to power system operators.

Nevertheless, predicting EGU emissions using public-only information accurately remains a challenging task. We have identified three main barriers to enhancing the EGU prediction accuracy, described as follows.

First, there are no effective tools to take advantage of the large number of datasets available in the public domain. For example, EGUs in the U.S. with a nameplate capacity over 25 MW equivalent (or combusting fuels with a sulfur content greater than 0.05% by mass) are required by law to be equipped with continuous emissions monitoring systems (CEMS). All data records collected by CEMS since 1990 are publicly available. However, our literature survey revealed that most of existing studies on predicting EGU emissions focused on a single unit using various data-driven techniques including autoregression,[2,3] neural networks,[4–9] SVM,[10,11] and ELM.[12] A commonality among these studies is access to detailed EGU operational data that exists outside of the public domain, which makes repeating or generalizing such approaches to other units infeasible. By contrast, only linear regression (LR) has been reported for modeling CEMS data from a large EGU fleet.

Second, previous efforts in EGU emission prediction have not taken advantage of all the relevant public datasets available besides the emission monitoring data such as CEMS. For example, while intended to facilitate field audits of facilities that report CEMS data, the USEPA Field Audit Checklist Tool (FACT) allows users to view not only CEMS data but also monitoring plans and quality assurance plans. Users can obtain the corresponding method of determination codes (MODC) for CEMS data to differentiate data points based on measurement from those based on calculations. Therefore, MODC provides further insight in interpreting CEMS data.

Third, predicting NO_x emissions, which are a direct public health concern in the form of NO_2, a criteria pollutant as well as a primary ozone precursor, presents additional challenge as emission control technologies, both combustion-based and post-combustion, affect NO_x emissions differently, and their effectiveness depends on EGU operating conditions as NO_x formation during combustion depends on complex chemical kinetics occurring within turbulent flows.[13,14] Therefore, the need for improving the prediction of NO_x emissions is imperative.

In this paper, we addressed the barriers described above by developing machine learning (ML)-based models to predict NO_x, SO_2, and CO_2 emission rates and utilizing a variety of public datasets in addition to CEMS data. We thoroughly evaluated the effectiveness of this approach by predicting emissions from all thermal EGUs larger than 25 MW in New York State (NYS) on a year-by-year and unit-by-unit basis with increasing prediction horizons and interpreted the modeling results utilizing permutation importance. NYS was chosen as the focal area in our study as the EGU fleet in NYS is large and diverse. The 328 thermal EGUs, span six generation types and eight fuel types providing opportunities for detailed unit-by-unit analyses. Furthermore, the power system in NYS became coal-free in 2020, foreshadowing the future generation mix across the U.S. We aimed to make these models transparent by using only publicly available data and generalizable among different units.

The paper is organized as follows. We first introduce the data collection (Section 2.1) and data cleaning process (Section 2.2), followed by a description of model implementation (Section 2.3). Then we describe the model evaluation procedure (Section 2.4) and the approaches used to analyze and interpret the models (Section 2.5). Finally, we show the model's predictive performance and analysis results (Section 3).

2 Methods

Fig. 1 shows the key steps of our study. The rest of Section 2 is structured to elaborate each of the key steps.

2.1 Data collection

We downloaded hourly, unit-level CEMS data for New York State (NYS) from 2015 to 2019 using the Air Markets Program Data (AMPD) tool[15] from USEPA. Among the variables in the raw CEMS data, we aimed to predict hourly emission rates of NO_x, SO_2, and CO_2. But these must be derived in different ways. The NO_x concentrations in ppm and diluent concentration in % O_2 or CO_2 are measured in a NO_x-diluent monitoring system,[16] and then the hourly NO_x emission rate in pounds per mmBtu is calculated.[17] The NO_x emission rate in pounds per hour is further calculated by multiplying the hourly NO_x emission rate in pounds per mmBtu by the reported hourly heat input in mmBtu per hour and the operating time.[17] The SO_2 emission rate in pounds per hour was estimated using the default SO_2 emission rate in pounds per mmBtu and the reported heat input rate in mmBtu per hour for most of the gas-fired units.[18] For the oil-fired units (and some of the gas-fired units), the SO_2 emission rate was calculated using the reported fuel consumption rate and the measured sulfur content.[18] The CO_2 emission rate in tons per hour was estimated using the recorded heat input rate in mmBtu per hour or quantified by a CO_2 monitoring system together with a flow monitoring system.[19] In the following discussion, we refer to these target variables as "CAMD-derived emission rates".

After removing non-contributing variables (i.e., those with constant or many missing values), we selected 16 features from the CEMS data for the predictive models, including month, hour, gross load, heat input, source category, SO_2 phase, NO_x

© 2023 The Author(s). Published by the Royal Society of Chemistry

Environ. Sci.: Adv., 2023, **2**, 1696–1707 | **1697**
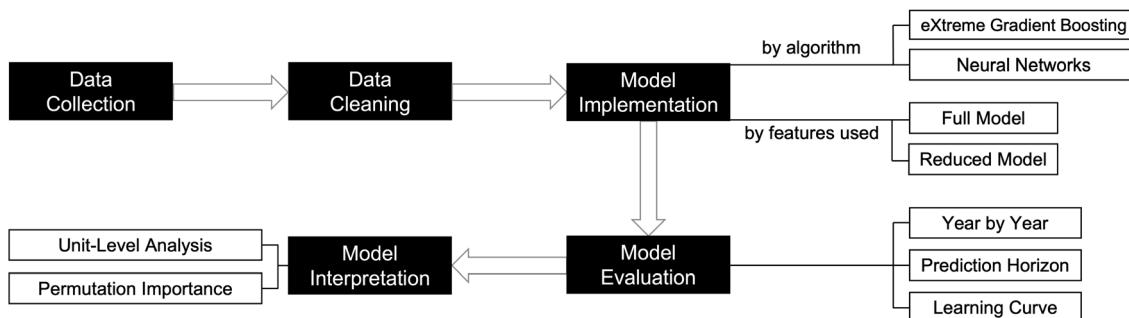
Fig. 1 Key steps in applying machine learning techniques to predict EGU emissions using public datasets.

phase, unit type, primary fuel type, secondary fuel type, SO_2 control, NO_x control, PM control, Hg control, facility latitude, and facility longitude. We added 4 additional features, which characterize EGU operational conditions, including the nameplate capacity, load range, hourly capacity factor, and hourly ramping factor. The nameplate capacity for each EGU and the hourly load range were collected using the USEPA Field Audit Checklist Tool (FACT). The hourly capacity factor and hourly ramping factor at hour t were calculated as follows:

Hourly capacity factor$_t$

$$= \frac{\text{gross load (MW)}_t \times \text{operating time (hour)}_t}{\text{nameplate capacity (MW)} \times 1 \text{ (hour)}}; \quad (1)$$

Hourly ramping factor$_t$

$$= \frac{\text{gross load (MW)}_{t-1} - \text{gross load (MW)}_t}{\text{nameplate capacity (MW)}} \quad (2)$$

The hourly load range, capacity factor, and ramping factor aim to train the models that higher emissions are likely to occur during part-load operation and ramping, respectively. In total, this resulted in 20 features. We then converted all the categorical features into numeric values using one-hot encoding, which converts one categorical value into a group of digits with a single "1" (hot) and all others "0" representing the same categorical value.

2.2 Data cleaning

For the NO_x emissions and heat input, we checked the corresponding method of determination codes (MODC) available using the USEPA FACT and removed substitute data points that were fully calculated instead of measurement-based. We deleted data points with no operating time or gross load as no emissions were generated during those conditions. We removed data points with partial operating hours to eliminate startup and shutdown conditions. Emissions associated with startup and shutdown conditions will be investigated in a future study.

In addition, we screened the heat rate (inverse of the thermal efficiency) data to identify anomalies. We identified three different heat rate regimes: $\sim$5000 Btu kW^{-1} h^{-1}, $\sim$7000 Btu kW^{-1} h^{-1}, and $\sim$10 000 Btu kW^{-1} h^{-1}. Note that 5000 Btu kW^{-1}

h^{-1}, or $\sim$70% thermal efficiency, is physically impossible for thermal EGUs and may indicate reporting errors. For example, Fig. 2 depicts hourly recorded heat input *versus* gross load in 2015, 2019, and 2021, respectively, for Unit 51RH at the Astoria Generating Station (Facility ID: 8906). It is a tangentially-fired unit with pipeline natural gas (PNG) as the primary fuel type. A majority of the data points fall into the $\sim$5000 Btu kW^{-1} h^{-1} heat rate regime, which was also reported in a 2018 study.[20] We conducted further investigation into this facility by examining its Title V permit from the New York Department of Environmental Conservation (NYSDEC). We gather that this unit is a twin-furnace boiler that exhausts emissions through two stacks, counted as two units (Unit 51RH and Unit 52SH). Therefore, we attribute these nonphysical heat rates to a systematic reporting error – or loophole. Specifically, dividing the gross load for the full boiler by the heat input for each individual furnace would halve the true heat rate, which could be the case here given the consistent trends shown in Fig. 2. In the current study, we removed data points with unrealistic heat rates (<6000 Btu kW^{-1} h^{-1}). For future study, we recommend stricter enforcement of data report procedures by USEPA to eliminate those reporting errors.

Finally, 253 479–329 202 effective data points remained for modeling depending on the year representing 113 units from four different unit types: combined cycle, combustion turbine, tangentially-fired, and dry bottom wall-fired boiler. Table 1 summarizes the 2018 statistics of NO_x emission rates for different unit types. Note that while the values in the table differ by year the order of magnitudes remain consistent.

2.3 Model implementation

We created two distinct ML-based models: a full model and a reduced model as illustrated in Fig. 3. The full model utilizes all the information contained in the public databases and is designed to be incorporated into a production cost model and/or serve as an electronic auditing tool to detect anomalies in the self-reported continuous emissions monitoring system (CEMS) data. This full model has the potential to facilitate power systems planning, identify regulatory compliance issues, improve data quality, and reduce emissions. The reduced model is designed to be linked to a power systems model to predict EGU emissions for air quality modeling. Since power systems models often rely on simplified network topologies, the reduced

© 2023 The Author(s). Published by the Royal Society of Chemistry

Name: Astoria Generating Station; Facility ID (ORISPL): 8906; Unit ID: 51RH;
Unit Type: Tangentially-Fired; Primary Fuel Type: Pipeline Natural Gas
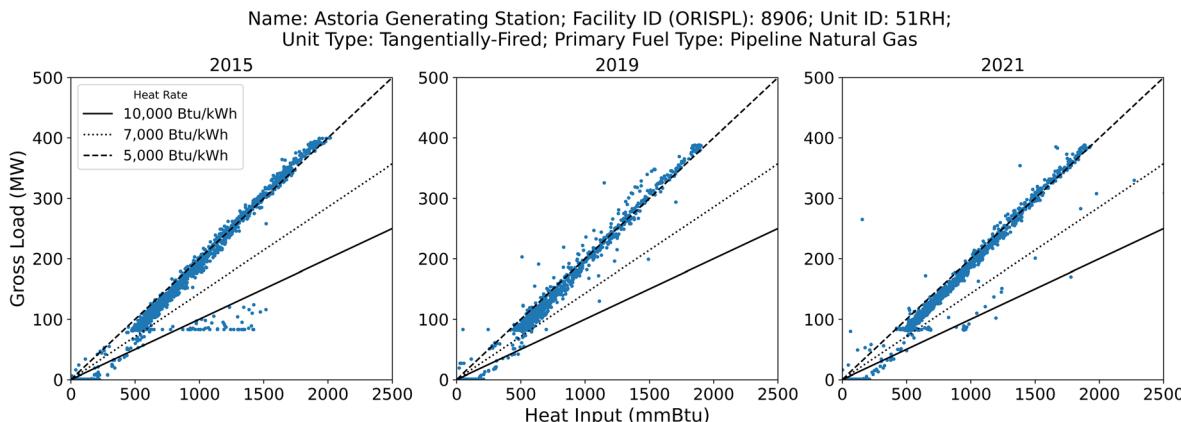
Fig. 2 The scatter plot of hourly recorded heat input *versus* gross load in 2015, 2019, and 2021, respectively, for the Unit 51RH at the Astoria Generating Station (Facility ID: 8906). Unit 51RH and Unit 52SH are two furnaces for the same boiler but the heat rates are reported by dividing the gross load for the full boiler by the heat input for each individual furnace, resulting in unrealistic values of around 5000 Btu kW^{-1} h^{-1}.

model only uses features that can be readily obtained from such power systems models.

2.3.1 Full models. The full model was built using historical data from all available units to predict the future EGU NO_x emission rate. Here "full" refers to the use of all 20 features (Fig. 3). Since the values of the NO_x emission rates were measurement-based, while the values of the SO_2 and CO_2 emission rates were mostly calculation-based (*i.e.*, calculated using other features and fuel properties), we included the SO_2 and CO_2 emission rates as additional features when predicting the NO_x emission rate, and did not implement full models for SO_2 and CO_2 emission rates.

Using linear regression (LR) as a benchmark, we screened several ML algorithms, including support vector machine (SVM), decision tree, adaptive boosting (AdaBoost), random forest (RF), extreme gradient boosting (XGBoost), and neural networks (NN), by comparing their full model performance. Among these algorithms, XGBoost and NN consistently outperformed the others. Therefore, we focused on XGBoost and NN for detailed analysis. All the models were implemented using the scikit-learn library in Python.[21] A brief description of XGBoost and NN is as follows.

XGBoost expands upon the principle of traditional gradient boosting algorithms, which iteratively combines weak learners

(*e.g.* shallow decision trees) into a strong learner to reduce the model bias and improve overall accuracy. It adds both L1 and L2 regulation to prevent model overfitting, and with the parallelization of individual tree building, offers improved computational efficiency as well.

The NN implemented in this study is a dense sequential (feed forward) neural network, which comprises two densely connected hidden layers, and an output layer that returns a single, continuous value. It is a multilayered perception model utilizing the back-propagation technique for training. The multiple layers and non-linear activation functions enable it to distinguish data that is not linearly separable.

2.3.2 Reduced models. Given that much of the power system is classified as critical infrastructure, detailed data about its operation can be difficult or impossible to obtain. In order to carry out medium- to long-term power systems planning studies and to tease out the sensitivities to current and future policies, researchers use publicly available reduced-form representations of the power system.[22] These network topologies can be used in unit commitment, economic dispatch, and optimal scheduling algorithms to determine operating set points for each EGU in the system. Reduced models aim to preserve load, flow, and congestion patterns on a system without disclosing critical infrastructure information. EGUs in reduced power system

Table 1 Statistical summary of the 2018 NO_x emission rates for different types of units (combined cycle, combustion turbine, tangentially-fired, and dry bottom wall-fired boiler), including the number of units, the number of data points, mean, standard deviation, 25th, 50th (median), 75th, 90th, and 100th (maximum) percentiles of the emission rate values (unit: pounds per hour)

Unit type	Number of units	Number of data points	Mean	Standard deviation	Percentile				
					25th	50th	75th	99th	100th
Combined cycle	56	214 580	19.8	20.3	7.7	12.5	23.9	89.1	621.8
Combustion turbine	29	30 099	13.0	19.2	3.6	4.1	26.1	43.9	302.0
Tangentially-fired	21	46 895	129.3	188.1	33.2	81.5	151.6	1116.5	2153.7
Dry bottom wall-fired boiler	6	3125	139.0	274.0	18.1	21.8	75.1	1296.3	2350.6

© 2023 The Author(s). Published by the Royal Society of Chemistry

Environ. Sci.: Adv., 2023, **2**, 1696–1707 | **1699**
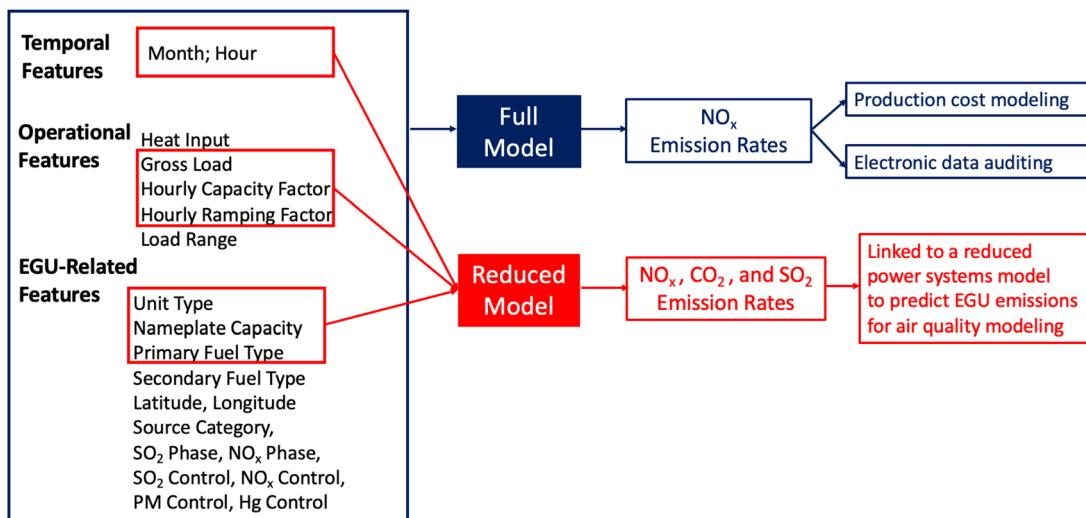
Fig. 3 Two distinct ML-based models, full model, and reduced model, for different applications.

models often represent many actual units aggregated by region, fuel type, unit type, or some combination of the three. Since these aggregated generators do not mirror those in the real world, emissions estimates become more challenging. Therefore, we implemented a reduced (emission) model to predict the NO_x emission rate that uses only eleven features including EGU-related features (*i.e.*, primary fuel type, unit type, and name-plate capacity), operational features (*i.e.*, operating time, gross load, hourly capacity factor, and hourly ramping factor), and temporal features (*i.e.*, hour and month) as shown in Fig. 3.

Considering that the heat input rate plays a key role in calculating the SO_2 and CO_2 emission rates and is typically not available in the reduced-form representations of the power system for a future scenario, we built reduced models to estimate the hourly heat input. Then we calculated the SO_2 and CO_2 emission rates using the equations specified in Appendix D to Part 75 of 40 CFR[18] (for the SO_2 emission rate) and Appendix G to Part 75 of 40 CFR[19] (for the CO_2 emission rate):

$$SO_2 \text{ emission rate (pounds per hour)} = 0.0006 \text{ pounds per mmBtu} \times \text{hourly heat input (mmBtu per hour)} \quad (3)$$

where 0.0006 pounds per mmBtu is the default SO_2 emission rate for the gaseous fuels. Note that we only calculated the SO_2 emission rate for gas-fired hours. For oil-fired hours, additional information about fuel properties (*e.g.* sulfur content) is needed, which can be specified for a future scenario.

$$CO_2 \text{ emission rate (tons per hour)}$$
$$= \frac{F_c \times \text{hourly heat input (mmBtu per hour)} \times U_f \times MW_{CO_2}}{2000} \quad (4)$$

where $MW_{CO_2} = 44.0$ pounds per pound-mole is the molecular weight of carbon dioxide; F_c is the carbon-based F-factor, equal to 1040 scf per mmBtu for the natural gas-fired units and 1420 scf per mmBtu for the oil-fired units; $U_f = 1/385$ scf CO_2 per pound-mole at 14.7 psia and 68 °F.

2.4 Model evaluation

We split the data into training and test sets in three different ways, which are depicted in Fig. 4. First, in order to test the forecasting ability of the model considering interannual variability, we implemented the models by training on the previous year's data and testing on the following year's data, year-by-year from 2015 to 2019. Second, in order to investigate how far ahead the model is capable of making predictions, we evaluated the model with different prediction horizons. Using the data from 2019 as the test set, we trained the model with the data from 2015 to 2018 (1 year prediction horizon), from 2015 to 2017 (2 year prediction horizon), from 2015 and 2016 (3 year prediction horizon), and with the data from 2015 (4 year prediction horizon). Note that the prediction horizon increases from 1 to 4 years. Third, in order to find the amount of training data needed to achieve optimal performance, we drew learning curves of model performance by training models with different amounts of data from a half-year to four years. Data were combined from the odd-numbered months (January, March, May, July, September, and November) to create the half-year.

To evaluate the models' performance, we employed the coefficient of determination (R^2), root mean square error (RMSE), and normalized RMSE (nRMSE) as the main metrics. R^2 measures the proportion of the variance that is explained by the model indicating how well the model replicates the data. RMSE measures the square root of the average squared difference between the predictions and observations. We normalized RMSE by the standard deviation, referred to as nRMSE, to take into account the slightly different scales of data points in different years.

2.5 Model interpretation

We conducted two independent analyses to characterize the models' predictive performance in terms of identifying key features and making meaningful representations from the data. First, we examined the model performance at the unit level. Second, we measured model feature importance using permutation importance[23] for all features in the full model. Briefly,
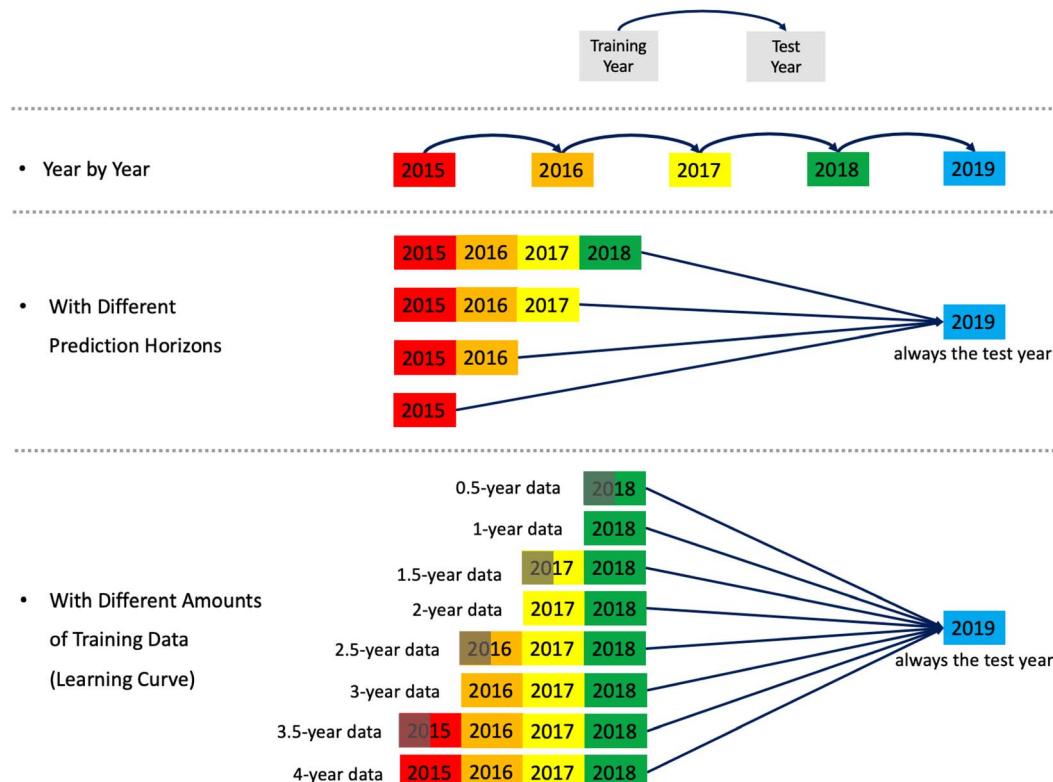
Fig. 4 Sketch of the model evaluation in tree different ways: year by year, with different prediction horizons, and with different amounts of training data (learning curve).

this method randomly shuffles a feature's value and determines the feature's importance based on the respective performance decrease. It is model-agnostic but note that the permutation importance can be misleading when features are highly correlated, resulting in lower importance values. Therefore, we only kept one feature among a group of correlated features (Pearson correlation coefficient >0.8) when calculating permutation importance and assigned the same permutation importance to all the correlated features within the group.

3 Results and discussion

3.1 Overall model predictive performance on NO_x emission rates

Table 2 summarizes the overall predictive performance of NO_x emission rates for the full and reduced models, respectively,

using the year-by-year evaluation approach. Both XGBoost and NN show strong overall predictive performance in terms of R^2, RMSE (pounds per hour), and nRMSE and outperform LR. In the full model (Table 2), the R^2 for LR is between 0.82 and 0.91 with nRMSE ranging from 0.011–0.012, while the R^2 for XGBoost and NN R^2 can achieve 0.95–0.96 with nRMSE ranging from 0.005–0.008. XGBoost and NN models perform similarly, with the difference in R^2 less than 0.01, in RMSE less than 1.4 pounds, and in nRMSE of less than 0.001. Both XGBoost and NN perform consistently in terms of R^2 and nRMSE for different training and test years with a one-year prediction horizon.

As shown in Table 3, XGBoost and NN for the reduced model, which contains far fewer features than the full model, still perform well with R^2 between 0.86–0.93 and nRMSE between 0.007–0.015. By contrast, LR performs poorly, with much lower R^2 between 0.29–0.54 and much higher nRMSE between 0.021–

Table 2 The LR, XGBoost, and NN predictive performance in terms of R^2, RMSE (pounds per hour), and nRMSE of full models on NO_x emission rates (trained on the previous year's data and tested on the following year's data, year-by-year from 2015 to 2019)

| Training year | Test year | Full model | | | | | | | | |
| | | LR | | | XGBoost | | | NN | | |
		R^2	RMSE	nRMSE	R^2	RMSE	nRMSE	R^2	RMSE	nRMSE
2015	2016	0.91	26.2	0.011	0.96	17.7	0.007	0.96	18.5	0.008
2016	2017	0.89	26.3	0.012	0.96	16.0	0.007	0.96	16.3	0.007
2017	2018	0.90	29.4	0.012	0.95	21.0	0.009	0.95	19.6	0.008
2018	2019	0.82	23.9	0.011	0.96	11.0	0.005	0.96	11.8	0.005

© 2023 The Author(s). Published by the Royal Society of Chemistry

Environ. Sci.: Adv., 2023, **2**, 1696–1707 | **1701**

Table 3 The LR, XGBoost and NN predictive performance in terms of R^2, RMSE (pounds per hour), and nRMSE of reduced models on NO_x emission rates (trained on the previous-year data and tested on the following-year data, year-by-year from 2015 to 2019)

Training year	Test year	Reduced model								
		LR			XGBoost			NN		
		R^2	RMSE	nRMSE	R^2	RMSE	nRMSE	R^2	RMSE	nRMSE
2015	2016	0.54	59.7	0.025	0.93	22.9	0.010	0.90	27.4	0.011
2016	2017	0.39	62.9	0.028	0.93	21.8	0.010	0.90	25.2	0.011
2017	2018	0.38	72.7	0.031	0.86	34.2	0.015	0.86	34.2	0.015
2018	2019	0.29	47.5	0.021	0.91	16.4	0.007	0.90	17.8	0.008

0.031. The reduced XGBoost models perform slightly better than the reduced NN models (*i.e.*, slightly higher R^2; slightly lower RMSE and nRMSE), with a difference in R^2 of less than 0.03, RMSE of less than 4.5 pounds, and nRMSE of less than 0.001. The reduced model is somewhat more sensitive to the chosen training and test years compared with the full model.

To summarize, compared with applying linear models, applying non-linear algorithms to predict the EGU NO_x emission rate can significantly enhance model performance and achieve much higher prediction accuracy, especially for models with fewer features.

3.2 Unit-level model predictive performance on NO_x emission rates

We use the full XGBoost model trained on 2017 data and tested on 2018 data as an example to investigate the details of model performance. Fig. 5a presents the scatter plots of CAMD-derived *vs.* predicted NO_x emission rates on different scales (2500 pounds per hour in the left plot and 500 pounds per hour in the right plot). About 99.4% of the NO_x emission rates fell below 500 pounds in 2018, *i.e.*, within the region shown in the right scatter plot. The overall trend follows the identity line indicating good overall model predictive performance ($R^2 = 0.95$, nRMSE =
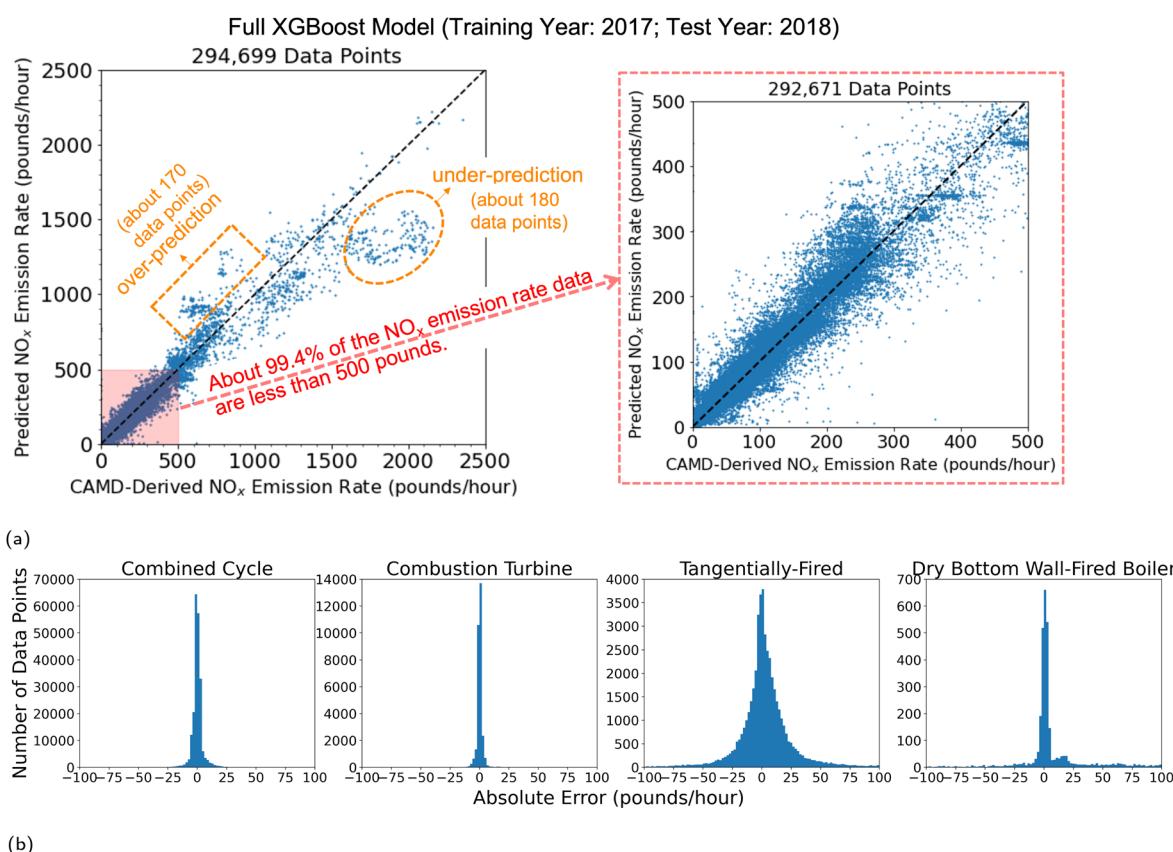
Fig. 5 Detailed prediction performance output from the full XGBoost model trained on 2017 data and tested on 2018 data: (a) the scatter plots of CAMD-derived *versus* predicted NO_x emission rates for the full XGBoost model in different scales: left = 2500 pounds; right = 500 pounds; (b) the distribution of absolute errors, *i.e.*, the difference between the predicted NO_x emission rates and the CAMD-derived NO_x emission rates, for different unit types (combined cycle, combustion turbine, tangentially-fired, and dry bottom wall-fired boiler).

0.009). Fig. 5b illustrates the corresponding distributions of the absolute errors, *i.e.*, the difference between the predicted NO_x emission rates and the CAMD-derived NO_x emission rates, grouped by different unit types including combined cycle, combustion turbine, tangentially-fired, and dry bottom wall-fired boiler. The absolute errors are concentrated around 0 for all unit types. But the tangentially-fired units have the widest error distribution as a result of much larger NO_x emission rates than the other types of units. As shown in Table 1, the NO_x emission rates from the tangentially-fired units averaged 120.0 pounds per hour, and some extreme values exceeded 2000 pounds per hour in 2018.

3.2.1 Combined cycle and combustion turbine units. NO_x emission rates from combined cycle and combustion turbine units fell within a much smaller range than tangentially-fired and dry bottom wall-fired boiler units. For combined cycle units, which contribute the majority (two-thirds) of the data points, approximately 99% of the NO_x emission rates were below 100 pounds per hour with a mean value of 19.8 pounds per hour (Table 1). More than half of the data points have an absolute error magnitude lower than 2 pounds per hour, and approximately 80% of the data points have an absolute error magnitude lower than 4 pounds per hour, as shown in Fig. 5b. For combustion turbine units, more than 99% percent of the NO_x emission rates were below 45 pounds per hour with a mean value of 13.0 pounds per hour (Table 1). Around 77% of the data points have an absolute error magnitude lower than 2 pounds per hour, and around 91% of the data points have an absolute error magnitude lower than 4 pounds per hour (Fig. 5b).

The models also captured the impact of emission control technologies. Fig. 6 compares the distributions of absolute prediction errors for combined cycle units equipped with selective catalytic reduction (SCR) and those with steam injection, using the full model (Fig. 6a) and the reduced model (Fig. 6b), respectively. Note that the steam injection units typically have much higher NO_x emission rates than the SCR units,

as SCR is more effective in reducing NO_x emissions than steam injection. All the distributions are centered around a zero mean, indicating that the models generally captured emission rate magnitude differences. Higher emission rates and more dynamic combustion conditions in the steam injection units led to higher prediction errors for these units than the SCR units.

3.2.2 Tangentially-fired units. There is a noticeable under-prediction zone highlighted by the orange dashed oval shown in the left scatter plot in Fig. 5a. Roughly 180 data points fall within this zone, and all of them come from a single facility: the Roseton Generating LLC facility in Newburgh, NY, which houses two tangentially-fired units (Facility ID: 8006; Unit ID: 1 and 2). In general, both units operated infrequently during the first quarter of the year (less than 100 hours). However, in January 2018, those two units operated at nearly full capacity for more than 250 hours leading to high NO_x emission rates (>1500 pounds per hour), which are shown for Unit 2 in the bottom plot of Fig. 7. The units are dual-fuel combustion turbines, with residual oil as the primary fuel and pipeline natural gas (PNG) as the secondary fuel. The ratios between CO_2 emissions and heat input, as shown in the upper plot of Fig. 7, suggest that fuel switching occurred. We identified two critical values for this ratio (essentially CO_2 emission factor), *i.e.*, 0.059 and 0.081 short tons per mmBtu, corresponding to natural gas and oil, respectively. Those two units burned residual oil in January and March while burning pipeline natural gas during the remainder of the year. This unusual operational paradigm was driven by a cold snap that occurred in early January 2018. According to the National Weather Service, temperatures across the majority of the central and eastern U.S., including NYS, averaged 10 to 25° below normal between late December 2017 and early January 2018.[24] The NYS-wide electricity load on January 5, 2018 nearly exceeded its historical winter peak. Therefore, these units burned residual oil, stored on-site to ensure reliability when cold temperatures create natural gas supply challenges. A time-
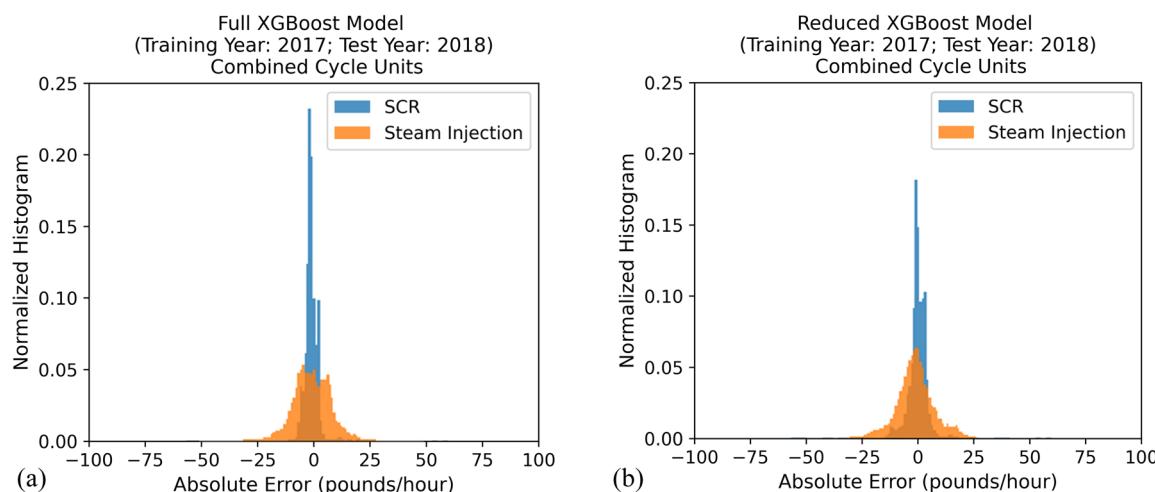
Fig. 6 The distribution of absolute errors, *i.e.*, the difference between the predicted NO_x emission rates and the CAMD–derived NO_x emission rates, for the combined cycle units with different NO_x control technologies (with SCR, steam injection) output from the (a) full XGBoost model; (b) reduced XGBoost model trained on 2017 data and tested on 2018 data.

© 2023 The Author(s). Published by the Royal Society of Chemistry

Environ. Sci.: Adv., 2023, **2**, 1696–1707 | **1703**
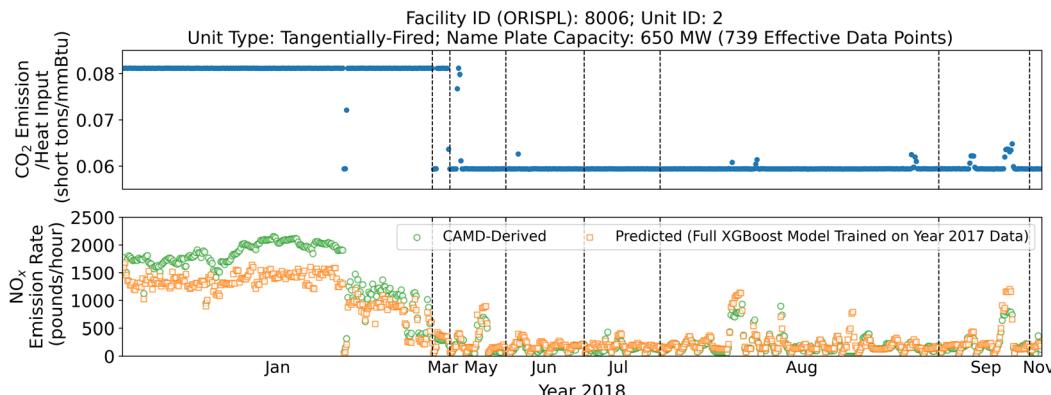
Fig. 7 The ratios between CO_2 emissions and heat input (upper), and CAMD-derived *versus* predicted NO_x emission rates (bottom, $R^2 = 0.86$) from Unit 2 of the Roseton Generating LLC facility in Newburgh, NY (Facility ID: 8006) in 2018, with abnormal high NO_x emission rates in January corresponded with the under-prediction zone shown in the left scatter plot in Fig. 5a.

series comparison of CMAD-derived and predicted emission rates for Unit 2 depicted in the bottom plot of Fig. 7, shows that the model did elevate predictions of NO_x emission rates in January but still under-predicted the exact values. The magnitude of the absolute error reached 804.8 pounds per hour. During other operational time periods for Unit 2, the model performed well pushing the unit-level R^2 to 0.86.

Another over-prediction zone highlighted by the orange dashed box in the left scatter plot in Fig. 5a, contains about 170 data points. Most of these come from one of the tangentially-fired units within the Ravenswood Generating Station in Long Island City, NY (Facility ID: 2500; Unit ID: 30). As shown in the bottom plot of Fig. 8, these mispredictions occurred in June, July, August, and September 2018 with NO_x emission rates (bottom plot) at relatively high levels. Although the unit uses residual oil as the primary fuel and PNG as the secondary fuel, the ratios between CO_2 emissions and heat input suggest that the unit was burning PNG most of the time in 2018 as shown in the upper plot of Fig. 8. When those mispredictions occurred, the ratios exceeded 0.059 (but remained below 0.081) indicating the supplement of residual oil, which results in the over-predictions

of these emission rates. During the remainder of the year, the model performed well with predicted rates following calculated rates closely resulting in a unit-level R^2 of 0.88.

In summary, for the tangentially-fired units with high NO_x emission rates, the model captures the correct temporal trend but mispredicts the magnitude of the emission rate when an EGU operates abnormally (*e.g.*, switches fuel or is co-fired with different fuels). Furthermore, it is very important to include both CO_2 and heat input as features to predict NO_x emissions.

3.3 Features' importance in predicting NO_x emission rates

We quantified feature importance for the full model using permutation importance. Permutation importance measures the decrease in model performance when randomly shuffling a feature's value. Using the full model for the NO_x emission rate trained on 2017 data and tested on 2018 data as examples, Fig. S1a in the ESI† ranked the feature importance for the full XGBoost model, and Fig. S1b† for the full NN model. The bars (corresponding to the left axis) represent the permutation importance of the top 20 features with each feature ranked from most to least important, and the blue dots and green triangles
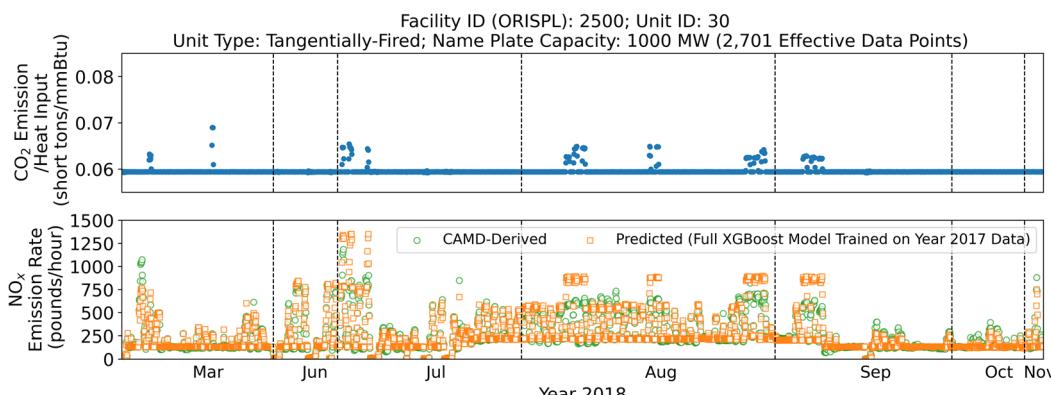

Fig. 8 The ratios between CO_2 emissions and heat input (upper), and CAMD-derived *versus* predicted NO_x emission rates (bottom, $R^2 = 0.88$) from Unit 30 of the Ravenswood Generating Station facility in Long Island City, NY (Facility ID: 2500) in 2018, with NO_x emission rates of about 160 data points over-predicted in June, July, August and September corresponded with the over-prediction zone shown in the left scatter plot in Fig. 5a.

(corresponding to the right axis) show the model performance in terms of R^2 for training data and test data, respectively.

Heat input, gross load, and CO_2 emission rates are the most influential features. With these three features, the test R^2 reaches 0.90 for the full XGBoost model and 0.86 for the full NN model. Notice that these three features are highly correlated, so when calculating the permutation importance, they were combined to form one group and assigned the same permutation importance.

For the full NN model, nameplate capacity and SO_2 emission rate rank fourth and fifth with relatively larger permutation importance values (>0.1) than the remaining features. For the full XGBoost model, SO_2 emission rate, tangentially-fired unit type, hourly capacity factor, and load range rank fourth – seventh with permutation importance values larger than 0.1. Historically, tangentially fired boilers were widely used in coal-fired power plants but were converted to burn natural gas as the primary fuel type in NYS. As mentioned in Section 3.2, the NO_x emissions from the tangentially-fired boilers were overall much higher than the other types of units. Therefore, the model is able to differentiate those units from the other types, and the corresponding features indicating this specific unit type show relatively high permutation importance.

3.4 Varying prediction horizon and learning curve for NO_x emission rates

Fig. S2a in the ESI† shows the model performance on 2019 data with prediction horizons increasing from 1 to 4 years. Overall, the model performance only deteriorates slightly when the prediction horizon increases. For example, with a 4 year prediction horizon, i.e., when the model was trained only using data from 2015, the model still achieves an acceptable range with R^2 ranging from 0.88 to 0.92 depending on the model type.

Fig. S2b in the ESI† depicts the model performance in terms of R^2 with respect to the amount of data used, starting with a half-year of data from 2018, and finishing with 4 years of data from 2015 to 2018. In all cases, the test data came from 2019. There is an increasing trend in R^2, though small, for each

addition of data to the training set. With a half-year of data from 2018, both the full and reduced models already achieve satisfactory performance, i.e., a full model R^2 larger than 0.93 and a reduced model R^2 larger than 0.87. For the XGBoost model, R^2 for the full model increases from 0.95 (trained with a half-year of data from 2018) to 0.96 when another half-year of data is added. It then remains at 0.96 even with all four years of data added. R^2 for the reduced XGBoost model increases from 0.87 to 0.90 going from a half-year to a full year of data and finally reaches 0.91 as more data are added. For the NN model, R^2 for the full model increases from 0.93 (trained with a half-year of data from 2018) to 0.94 with the full year of data added, and finally reaches 0.96 with all four years of data. R^2 for the reduced NN model increases from 0.87 (trained with a half-year of data from 2018) to 0.91 with all four years of data. A deviation from the increasing trend in model performance occurs for the NN models when the 2016 data are added.

3.5 Reproducing SO_2 and CO_2 emission rates with predicted hourly heat input

As denoted in eqn (3) and (4), the SO_2 and CO_2 emission rates are derived based on heat input. Therefore, in order to reproduce the SO_2 and CO_2 emission rates for the reduced model, we implemented an additional reduced model to predict the hourly heat input. The model was trained on the previous year's data and tested on the current year's data, year by year from 2015 to 2019. Both XGBoost and NN models show strong overall predictive performance in terms of R^2 (0.98–0.99). Fig. 9a shows a scatter plot of the measured vs. predicted hourly heat input from the reduced XGBoost model for heat input trained on 2017 data and tested on 2018 data as an example.

We then calculated the SO_2 emission rates (for gas-fired hours only) and CO_2 emission rates using eqn (3) and (4), respectively, and the predicted hourly heat input. Fig. 9b and c show CAMD-derived vs. predicted SO_2 and CO_2 emission rates, respectively, for 2018. The models for SO_2 and CO_2 both perform well, which strongly depend on the predicted hourly heat input.


(a) (b) (c)
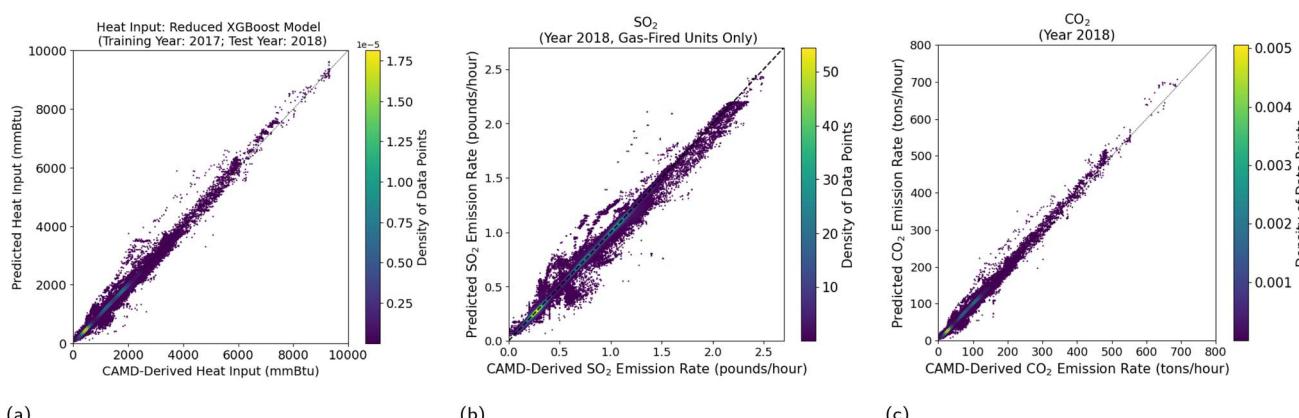
Fig. 9 The scatter plot of (a) measured versus predicted hourly heat input from the reduced XGBoost model (trained on 2017 data and tested on 2018 data); (b) CAMD-derived versus predicted SO_2 emission rates for gas-fired hours only, with the predicted values calculated by eqn (3) using the predicted hourly heat input; (c) CAMD-derived versus predicted CO_2 emission rates, with the predicted values calculated by eqn (4) using the predicted hourly heat input.

4 Conclusions

Predictive models of emissions from electric generating units are used in a wide range of important energy and environmental applications. Driven by a need for improved emissions predictions, we developed machine learning-based models to predict the emission rates of several pollutants using a variety of publicly available datasets. The models achieved an unprecedented high level of performance. For example, the R^2 value for NO_x emission rates reached as high as 0.96 and 0.93 for both the full and reduced models, respectively. These models also show the capability of differentiating NO_x control technologies. In order to reproduce calculation-based SO_2 and CO_2 emission rates, we built a reduced model to estimate the heat input, which plays a key role in calculating the SO_2 and CO_2 emission rates. Both XGBoost and NN models show strong overall predictive performance with R_2 reaching 0.95–0.99. Those results demonstrated that our proposed strategies, *i.e.*, applying machine learning techniques and using diverse datasets, have been effective. To the best of our knowledge, we were able to present in this paper the most accurate open-accessible unit-level emission prediction models for researchers, practitioners, and policymakers.

There are a number of future steps to further enhance our capability in predicting unit-level emissions. First, we identified and removed the data points with unrealistic heat rates (Section 2.2). Resolving the corresponding data issue by strictly enforcing the reporting protocols is important for improving the data quality. Second, we excluded the data points associated with the generator startup and shutdown in this study. Such conditions only accounted for about 5% of the entire dataset. However, startup or shutdown can lead to exceedingly high emission rates (and only last for a short period of time), making them worthy of a dedicated study. Third, the methodology presented in this paper can be readily applied to other regions. Our study focused on the generation fleet in New York State. This focused approach enabled us to conduct detailed unit-by-unit analyses and seek advice from state experts. Our overall approach can be readily implemented for modeling power plant emissions in other regions in the U.S., and it is generally applicable to other countries where public datasets of power plant emissions are available. Expanding the work to other regions will create a larger dataset, which should further improve the accuracy of the models. Finally, we found that the USEPA Field Audit Checklist Tool (FACT) provides valuable information, including additional generator characteristics, operating conditions, and methods of data determination, that are not available from the Air Markets Program Data (AMPD) tool. Follow-up studies that fully take advantage of the information presented in FACT, or any other informative features available from the public domain (*e.g.*, the generator model year), can provide additional insight into predicting unit-level emissions.

Conflicts of interest

There are no conflicts to declare.

Acknowledgements

References

1 E. Kahn, *Oper. Res.*, 1995, **43**, 388–398.

2 Y. Tunckaya and E. Koklukaya, *J. Energy Inst.*, 2015, **88**, 118–125.

3 S. M. Safdarnejad, J. F. Tuttle and K. M. Powell, *Comput. Chem. Eng.*, 2019, **124**, 62–79.

4 J. Song, C. E. Romero, Z. Yao and B. He, *Knowl Based Syst.*, 2016, **118**, 4–14.

5 F. Wang, S. Ma, H. Wang, Y. Li and J. Zhang, *Control Eng. Pract.*, 2018, **80**, 26–35.

6 P. Tan, B. He, C. Zhang, D. Rao, S. Li, Q. Fang and G. Chen, *Energy*, 2019, **176**, 429–436.

7 D. Adams, D.-H. Oh, D.-W. Kim, C.-H. Lee and M. Oh, *J. Cleaner Prod.*, 2020, **270**, 122310.

8 X. Hu, P. Niu, J. Wang and X. Zhang, *Atmos. Pollut. Res.*, 2020, **11**, 1084–1090.

9 G. Yang, Y. Wang and X. Li, *Energy*, 2020, **192**, 116597.

10 Y. Lv, J. Liu, T. Yang and D. Zeng, *Energy*, 2013, **55**, 319–329.

11 J. F. Tuttle, L. D. Blackburn and K. M. Powell, *Comput. Chem. Eng.*, 2020, **141**, 106990.

12 P. Tan, J. Xia, C. Zhang, Q. Fang and G. Chen, *Energy*, 2016, **94**, 672–679.

13 S. Hill and L. D. Smoot, *Prog. Energy Combust. Sci.*, 2000, **26**, 417–458.

14 P. Glarborg, J. A. Miller, B. Ruscic and S. J. Klippenstein, *Prog. Energy Combust. Sci.*, 2018, **67**, 31–68.

15 United States Environmental Protection Agency (EPA), *Washington, DC: Office of Atmospheric Programs, Clean Air Markets Division*, available from EPA's Air Markets Program Data web site: **https://ampd.epa.gov**, accessed Aug, 2020.

16 Office of the Federal Register National Archives and Records Administration, *40 CFR Part 75.10 – General operating requirements*, available from: **https://www.law.cornell.edu/cfr/text/40/75.10**, accessed Aug, 2020.

17 Office of the Federal Register National Archives and Records Administration, *40 CFR Subpart H – NOX Mass Emissions Provisions*, available from: **https://www.law.cornell.edu/cfr/text/40/part-75/subpart-H**, accessed Aug, 2020.

18 Office of the Federal Register National Archives and Records Administration, *40 CFR Appendix D to Part 75 – Optional SO2 Emissions Data Protocol for Gas-Fired and Oil-Fired Units*, available from: **https://www.law.cornell.edu/cfr/text/40/appendix-D_to_part_75**, accessed Aug, 2020.

19 Office of the Federal Register National Archives and Records Administration, *40 CFR Appendix G to Part 75 – Determination of CO2 Emissions*, available from: **https://www.law.cornell.edu/cfr/text/40/appendix-G_to_part_75**, accessed Aug, 2020.

20 M. Rossol, G. Brinkman, G. Buster, P. Denholm, J. Novacheck and G. Stephen, *Environ. Sci. Technol.*, 2019, **53**, 13486–13494.

21 F. Pedregosa, G. Varoquaux, A. Gramfort, V. Michel, B. Thirion, O. Grisel, M. Blondel, P. Prettenhofer, R. Weiss, V. Dubourg, J. Vanderplas, A. Passos, D. Cournapeau, M. Brucher, M. Perrot and E. Duchesnay, *J. Mach. Learn. Res.*, 2011, **12**, 2825–2830.

22 M. V. Liu, B. Yuan, Z. Wang, J. A. Sward, K. M. Zhang and C. L. Anderson, *IEEE Trans. Power Syst.*, 2023, **38**(4), 3293–3303.

23 A. Altmann, L. Toloşi, O. Sander and T. Lengauer, *Bioinformatics*, 2010, **26**, 1340–1347.

24 National Oceanic and Atmospheric Administration, *Record Breaking Artic Cold December 26, 2017 – January 8*, 2018, available from: **https://www.weather.gov/okx/RecordCold_Dec17Jan18/**, accessed Aug, 2020.

© 2023 The Author(s). Published by the Royal Society of Chemistry

Environ. Sci.: Adv., 2023, **2**, 1696–1707 | **1707**